



# High performance forward osmosis cellulose acetate (CA) membrane modified by polyvinyl alcohol and polydopamine

Hai-ming Song<sup>1</sup> · Li-jing Zhu<sup>1</sup> · Zhi-xiang Zeng<sup>1</sup> · Qun-ji Xue<sup>1</sup>

Received: 6 November 2017 / Accepted: 20 June 2018 / Published online: 29 June 2018  
© Springer Nature B.V. 2018

## Abstract

Cellulose acetate (CA) is a low cost and readily available material widely used in forward osmosis (FO) membranes. However, the performance of pure CA membranes is not good enough in salt separation and the traditional modification methods are generally multistep and difficult to control. In this paper, we reported high performance cellulose acetate (CA) composite forward osmosis (FO) membranes modified with polyvinyl alcohol (PVA) and polydopamine (PDA). PVA was first cross-linked onto the surface of CA membranes, and then PDA was coated with a rapid deposition method. The membranes were characterized with respect to membrane chemistry (FTIR and XPS), surface properties comprising wettability (by water contact angle), and osmosis performance. The modified membrane coated by PVA and PDA shown better hydrophilicity and exhibited 16.72 LMH osmotic water flux and 0.14 mM reverse solute flux with DI water as feed solution and 2.0 M NaCl as draw solution and active layer facing the feed solution. This simple and highly effective modification method makes it as an excellent candidate for further exploration for FO.

**Keywords** FO membranes · Reverse solute diffusion · Polydopamine · Polyvinyl alcohol

## Introduction

Today, the world is experiencing one of its most severe water shortages. Membrane separation technology as a favorable prospect in desalination and sewage treatment has become the most promising approach to deal with the global water crises problem [1]. Forward osmosis (FO) is one of the most potential separation technologies for its green, low cost and low fouling tendency [2]. FO is an osmotically-driven membrane process, in which water transfers through a semi-permeable membrane from a lower concentrated feed solution to a higher concentrated draw solution due to osmotic pressure difference [3, 4]. It can be applied in various environmental

and industrial applications including seawater desalination [5, 6], municipal wastewater reclamation [7–9], food processing [10, 11] and industrial wastewater treatment [12–14].

In recent years, FO membranes have been made by the non-solvent induced wet-phase inversion approach [15–17] and interfacial polymerization (IP) [18–20]. During the phase-inversion process, the structure of the membrane is controlled by both the thermodynamics of the casting solution and the kinetics of transport process [21]. Wang et al. fabricate a double-skinned cellulose acetate membrane through phase inversion and thermal annealing; this membrane can mitigate the internal concentration polarization by preventing the salt and other solutes in the draw solution from penetrating into the membrane porous support [17]. However, phase-inversion process is hard to reach high performance FO membrane. IP is a well-established method to prepare the dense and thin active layer for thin film composite (TFC) membranes with good perm-selectivity, chemical resistance, and mechanical properties [22]. Wang et al. fabricated high-performance FO membranes through the interfacial polymerization reaction on polyethersulfone (PES)/sulfonated polysulfone (SPSf)-alloyed porous membrane. The FO membrane achieved a higher water flux of 69.8 LMH when against deionized water [23]. Wang et al. prepared FO membranes via second interfacial polymerization (SIP).

✉ Li-jing Zhu  
zhulijing@nimte.ac.cn

✉ Zhi-xiang Zeng  
zengzhx@nimte.ac.cn

<sup>1</sup> Key Laboratory of Marine Materials and Related Technologies, Zhejiang Key Laboratory of Marine Materials and Protective Technologies, Ningbo Institute of Materials Technology and Engineering, Chinese Academy of Sciences, Ningbo 315201, People's Republic of China

They reported that SIP with aliphatic diamine is an effective strategy to improve the FO membrane performance, such as high permeability, selectivity and antifouling tendency [24]. But, the cost of IP is high because acyl chloride is used in the reaction [25–27]. Therefore, a simpler and controllable method is expected to prepare FO membrane with high water flux and low solute flux.

Cellulose acetate (CA), as low cost and readily available material, has been successfully used for the fabrication of FO membranes [28–30]. However, performance of pure CA membrane is always not good enough to use in membrane separation. In this study, we provide a simple, fast and effective way to make a high-performance FO membrane with CA as substrate membrane. Polyvinyl alcohol (PVA), which is water soluble and nontoxic, was used to build a dense layer on the surface of CA membrane with crosslinking agent. Then PDA layer was coated with an accelerated polymerization process. Morphologies, chemical compositions, hydrophilicity, permeability and salt rejection of the FO membranes were investigated. This method to modified high performance FO membrane can be widely used in source water purification and seawater desalination.

## Experimental

### Materials

CA was purchased from Solvay, US and dried at 80 °C for 24 h. Glutaraldehyde (GA), polyvinyl alcohol (PVA), tris (hydroxymethyl) aminomethane hydrochloride (Tris), dopamine (DA), 1,4-dioxane, acetone and lactic acid were used directly and purchased from Aladdin, China. Polyethylene terephthalate (PET) fabric was bought from Hangzhou HC Filtration CO., LTD. Other reagents, such as ethanol and methanol, were bought from Sinopharm Chemical Reagent CO., LTD., China and used without further purification.

### Membrane preparation and modification

CA membranes were prepared via non-solvent induced phase separation and further modified with PVA and PDA by surface coating technology. CA solution was obtained by dissolving CA (14 g) in 1,4-dioxane (57 mL) and acetone (18.5 mL) at 60 °C. After releasing bubbles, the solution was casted onto a PET fabric and immersed into a water bath at room temperature for 2 h to thoroughly remove solvents. Then CA membranes were taken out and dipped into PVA solution at 60 °C for 5 min. After drying, the modified membranes were further cross-linked by immersing into GA solution (2 wt%). PVA modified CA membranes were named CA-V0.5 and CA-V3

respectively, in which the numbers denoted the concentration of PVA solution. Finally, PDA was deposited onto CA-V3. Briefly, CA-V3 was immersed into a freshly prepared DA solution (2 g/L) in Tris buffer solution (pH = 8.5, 50 mM) using CuSO<sub>4</sub> (5 mM)/H<sub>2</sub>O<sub>2</sub> (19.6 mM) as a trigger [31]. After 10 min, the sample was washed by water overnight and dried in a vacuum at 30 °C for 4 h and named as CA-V3-D.

### Membrane characterization

Membrane morphologies were observed by field emitting scanning electronic microscopy (SEM, Hitachi S-4800, Japan). The surface chemical compositions of the CA membranes before and after surface modification were analyzed using attenuated total reflectance Fourier transform infrared spectra (ATR-FTIR, Thermo-Nicolet 6700, America) and X-ray photoelectron spectroscopy (XPS, PHI 5300 ESCA System, Perkin-Elmer Co., America) employing Al K $\alpha$  excitation radiation (1486.6 eV) and a take-off angle of 45°.

### Wettability measurements

The hydrophilicity of the membranes was characterized by water contact angle measurements (CA, OCA20, Data physics, Germany). A piece of 1 × 5 cm<sup>2</sup> membrane sample was attached onto a glass slide and 2.0  $\mu$ L distilled water was dropped onto the air-side surface of the membrane at room temperature. The water contact angle decaying with drop age was recorded by speed optimum video measurement technology. At least five measurements were averaged to get a reliable value.

### FO performance

Deionized water and sodium chloride solution (2 mol/L) were used as feed solution and draw solution, respectively. Feed and draw solution reservoirs were placed on weighing

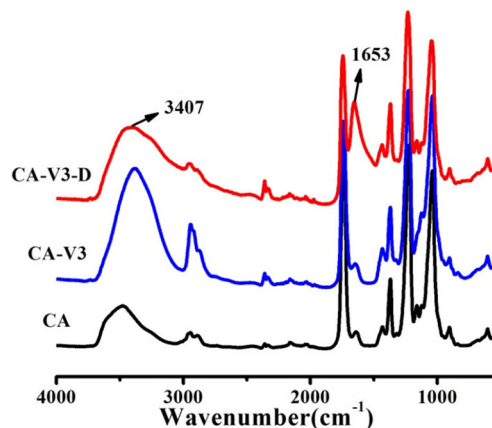
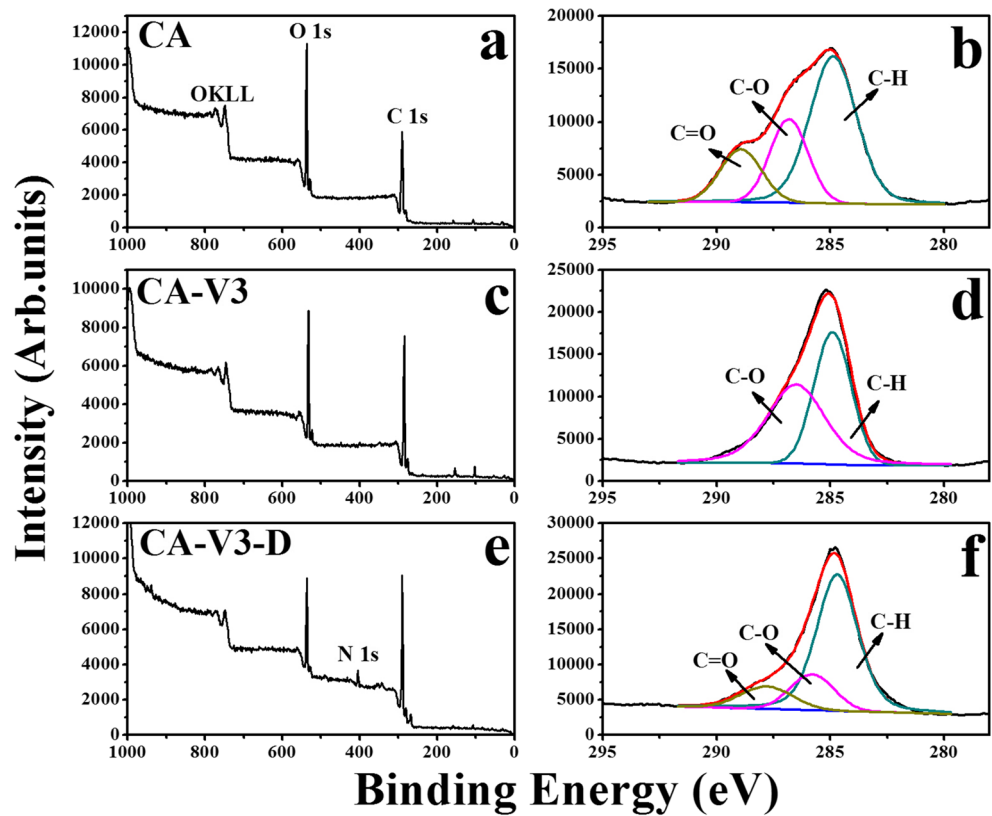


Fig. 1 ATR-FTIR spectra of CA, CA-V3 and CA-V3-D

**Fig. 2** Wide XPS spectra and C detailed spectra of (a, b) CA, (c, d) CA-V3 and (e, f) CA-V3-D



balances and were circulated at a rate of  $6.5 \pm 0.5 \text{ L} \cdot \text{h}^{-1}$  in a closed loop using gear pumps. All the experiments were conducted at  $25 \text{ }^\circ\text{C}$  with draw solution on the active side of the membrane. The water flux ( $J_w$ ,  $\text{L m}^{-2} \text{ h}^{-1}$ , abbreviated as LMH) is calculated from the volume change of the feed or draw the solution by Eq. (1).

$$J_w = \frac{\Delta V}{\Delta t} \frac{1}{A} \tag{1}$$

where  $\Delta V$  (L) is the volume change of feed solution,  $\Delta t$  (h) is the measuring time interval and  $A$  is an effective membrane area ( $0.0062 \text{ m}^2$ ).

The salt concentration in the feed water solution was determined from the conductivity measurement based on the standard concentration conductivity curve for NaCl. The reverse salt diffusion ( $J_s$ ,  $\text{mol m}^{-2} \text{ h}^{-1}$ , abbreviated as mMH) from the draw solution to the feed side was determined from the increase of the feed conductivity using the following Eq. (2):

$$J_s = \frac{(C_t V_t) - (C_0 V_0)}{\Delta t} \frac{1}{A} \tag{2}$$

where  $C_0$  and  $V_0$  are the salt concentration and the volume of the feed at the beginning;  $C_t$  and  $V_t$  are the salt concentration and the volume of the feed after  $t$  h. The mean data of at least three tests were reported for each membrane sample.

## Results and discussion

### Surface chemistry

Figure 1 shows the ATR-FTIR spectra of CA, CA-V3 and CA-V3-D. Compared with the original CA membrane, the peak at  $3407 \text{ cm}^{-1}$  (-OH resonance vibrations) of CA-V3 increases obviously. It verified the existence of PVA coating on the membrane surface. For the modified membrane of CA-V3-D, the peak at  $1653 \text{ cm}^{-1}$  (C=C resonance vibrations in aromatic ring) of CA-V3-D increases, while the peak at  $3407 \text{ cm}^{-1}$  decreases. The results confirmed that PDA has been coated on the membrane.

XPS was utilized to further study the chemical composition of the CA substrate and modified composite membranes. The wide scans and C 1 s core-level spectra are shown in Fig. 2. In comparison with the wide scan

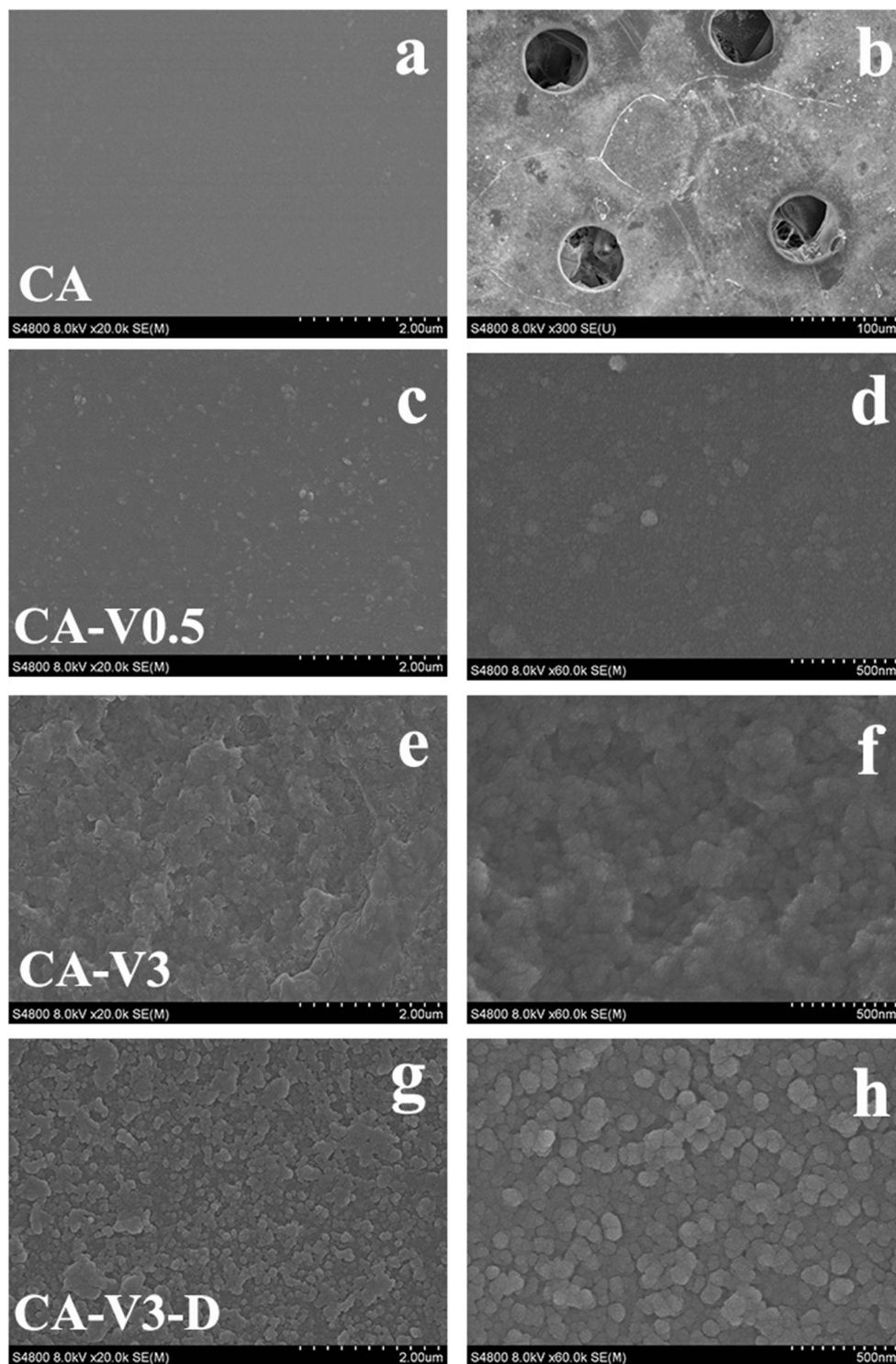
**Table 1** Elemental compositions of CA, CA-V3 and CA-V3-D

Sample	C (mol %)	O (mol %)	N (mol %)	O/C
CA	62.36	37.64	–	0.60
CA-V3	70.05	29.95	–	0.43
CA-V3-D	70.08	24.45	5.47	0.35

spectrum of CA and CA-V3, there is a new N 1 s signal at about 400 eV in the wide scan spectra of the CA-V3-D membrane surface. C 1 s core-level spectra of the membranes were collected and curved-fitted as shown in Fig. 2. C 1 s core-level spectrum of CA membrane is curved-fitted into C-C/C-H, C-O and C=O peaks at about 284.7, 285.8 and 288.8 eV, respectively. After

coating PVA, the C=O peak in the core-level spectrum of CA-V3 has disappeared, indicating PVA layer has been covered on the membrane surface completely. When DA was further deposited onto the membrane surface, C=O peak reappears as shown in Fig. 2f. The elemental molar percentages are shown in Table 1. It can be seen that the elemental contents of O in the membrane

**Fig. 3** SEM images of (a) the top surface of CA, (b) the bottom surface of CA, the top surface of (c, d) CA-V0.5, (e, f) CA-V3 and (g, h) CA-V3-D



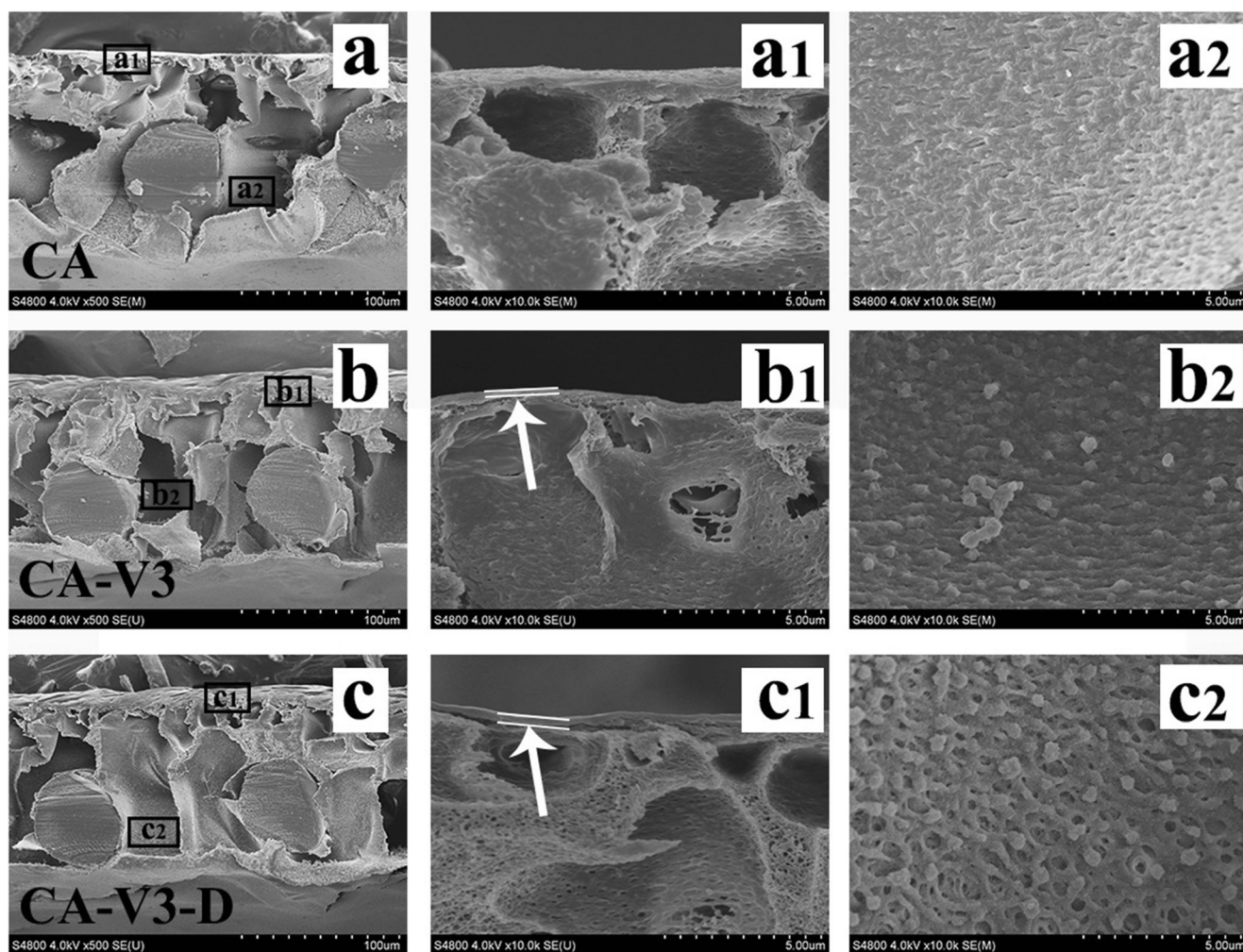


Fig. 4 Cross section SEM images of (a, a1, a2) CA, (b, b1, b2) CA-V3 and (c, c1, c2) CA-V3-D

surface of CA, CA-V3 and CA-V3-D are 37.64, 29.95 and 24.45 mol%, respectively. Meanwhile, the O/C ratio of CA-V3 decreases from 0.60 to 0.43 compared with CA which attributes the coating of PVA. Further, it drops down to 0.35 when PDA introduced onto the membrane.

XPS results confirmed that PVA and PDA were successfully covered on CA membranes.

### Morphologies of the membranes

The surfaces morphologies of CA, CA-V0.5, CA-V3 and CA-V3-D have been shown in Fig. 3. As shown in Fig. 3, the top surface of CA is flat and smooth without obvious microspheres. And it can be found that there are some pores at the bottom surface of the membrane. After surface modification, the surfaces of the membranes became irregular. Specially, after deposition of DA, plenty of PDA particles appeared on the membrane surface [32–34]. In addition, the cross-section structure of CA, CA-V3 and CA-V3-D are imaged in Fig. 4. It can be seen a dense top layer and a finger-like structure. The thickness of top layer for CA membrane is about 0.3 µm. After modification, a new coating layer can be seen and the thickness of the coating layer for CA-V3 and CA-V3-D is about 0.04 and 0.06 µm, respectively. The interior of cross-section displays microspheres structure and there are plenty of particles

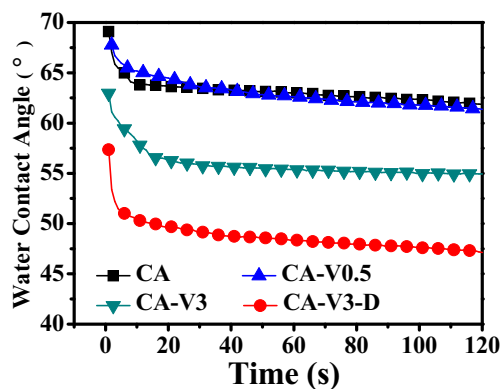
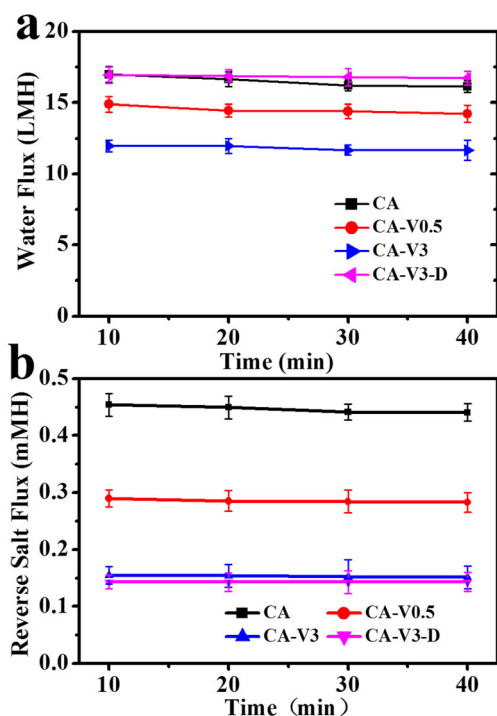


Fig. 5 The typical curves of water contact angle decaying with drop age for CA, CA-V0.5, CA-V3 and CA-V3-D



**Fig. 6** The osmotic water flux (a) and reverse salt flux (b) of CA, CA-V0.5, CA-V3 and CA-V3-D

on the pore walls of the modified membranes. The phenomena indicated that the surface and internal pore walls of CA membranes were modified by PVA and PDA via surface coating technique.

### Hydrophilicity of membranes

The water contact angles (WCA) of CA, CA-V0.5, CA-V3 and CA-V3-D are shown in Fig. 5. Compared with CA, WCA of CA-V0.5 changes little; WCA of CA-V3 becomes lower. In addition, the hydrophilicity of CA-V3-D further increases owing to the introduction of hydrophilic PDA on the membrane surface. For the dynamic contact angle of water, WCA of all the membranes decreases significantly in the first 10s and then declines slowly. After 120 s, WCA of the membranes are 67.77, 61.38, 54.93 and 47.12°, respectively. The results

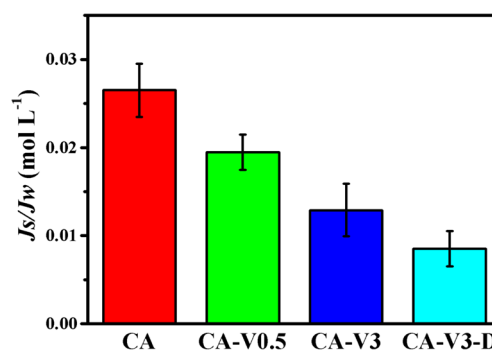


**Fig. 8** The  $J_s/J_w$  ( $\text{mol L}^{-1}$ ) value of CA, CA-V0.5, CA-V3 and CA-V3-D

indicated that the hydrophilicity of the modified membrane has been improved by the hydrophilic groups and CA-V3-D shown the best hydrophilicity for the introduction of PDA.

### FO performance of membranes

Figure 6 gives water flux ( $J_w$ ) and reverse salt flux ( $J_s$ ) of CA, CA-V0.5, CA-V3 and CA-V3-D. The  $J_w$  and  $J_s$  changes little with the increase of testing time and reach a stable state in 40 min. As shown in Fig. 6a, the PVA layer may affect the permeability of the membrane and made a decline of the water flux. CA-V3 shows a reduced water flux (11.66 LMH) than that of pristine CA membrane (16.10 LMH). However, when PDA was introduced on the surface, the water flux of CA-V3-D increased to 16.72 LMH. The reverse salt flux of CA, CA-V0.5, CA-V3 and CA-V3-D is 0.44, 0.28, 0.15 and 0.14 mMH, respectively. The illustration of the membranes was shown in Fig. 7. It can be seen that pure CA has poor property of salt and water rejection. After coating of PVA, PVA was crosslinked into a dense network with GA as the crosslinking agent. The dense layer can effectively increase the salt rejection but the water flux also decreased. However, when introduced PDA layer, the hydrophilicity of the membrane show a noticeable improvement, the water flux and reverse salt flux all improved compared with pure CA membrane.

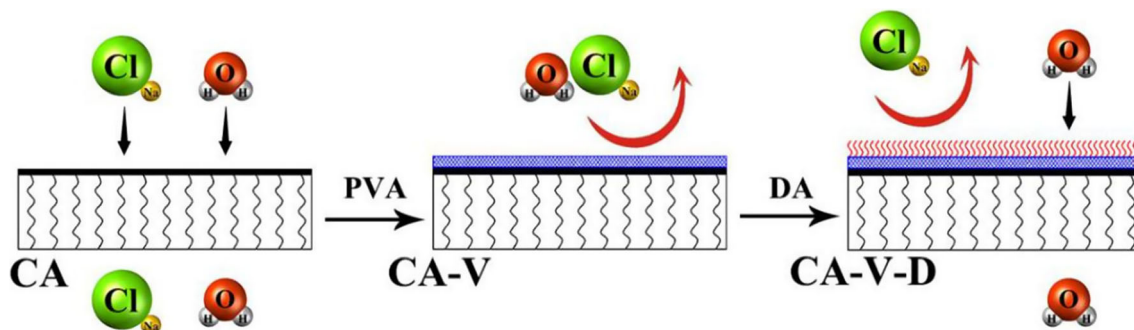


**Fig. 7** Illustration for the modification of CA FO membranes

**Table 2** Comparison of the FO performance for the modified CA membranes with literature data

Structure	FO performance		Testing conditions		Reference
	Water flux (LMH)	NaCl rejection (%)	Feed solution	Draw solution	
CA flat-sheet membrane	16.1	88.6	DI water	2.0 M NaCl	This work
CA-V3-D flat-sheet membrane	16.7	96.4	DI water	2.0 M NaCl	This work
CTA-W (HTI)	14.0	–	10 mM NaCl	1.0 M NaCl	[37]
Commercial cellulose triacetate with a cast nonwoven (CTA-NW) (HTI)	14.0	68.7	DI water	2.0 M NaCl	[38]
Commercial cellulose triacetate with an embedded polyester screen(CTA-ES) (HTI)	10.0	82.3	DI water	2.0 M NaCl	[38]
Thin-film composite with embedded polyester screen (TFC-ES) (HTI)	11.0	51.8	DI water	2.0 M NaCl	[38]

Specific salt flux,  $J_s/J_w$ , is a metric that is used to determine the amount of draw solute lost per unit of water that crosses the membrane. Lower  $J_s/J_w$  is desirable to prevent the loss of solutes [35, 36]. The  $J_s/J_w$  of the membranes is shown in Fig. 8. It can be seen that  $J_s/J_w$  of PVA modified membranes is lower than that of CA and it reduced from 0.0265 to 0.0195 and 0.0129 mol L<sup>-1</sup>. Specifically,  $J_s/J_w$  of CA-V3-D achieves 0.0085 mol L<sup>-1</sup>, which is 3 times lower than that of CA. This can prove that surface coating of PVA and PDA is an effective way to prevent losing the draw solute. A comparison of the FO performance of membranes synthesized in this work with some commercial membranes reported in literature is tabulated in Table 2. An ideal FO membrane shall possess high water flux and salt rejection. As compared with the reported CA membranes listed in the table, CA-V3-D synthesized in this work achieves comparable higher water flux and better salt rejection. NaCl rejection of CTA-NW, CTA-ES, TFC-ES made in Hydration Technologies Inc. (HTI) is only 68.7, 82.34 and 51.78, respectively. Due to its high FO performance, CA-V3-D is considered as an excellent candidate for further exploration as a membrane for FO.

## Conclusion

High performance FO membranes were made via a simple and effective method by introduction PVA and PDA layers on the surface of CA. PVA layer can effectively enhance the salt rejection but the osmotic water flux of the membrane had a little reduction. When hydrophilic PDA layer was further coated, the membrane shows the best FO performance with 16.72 LMH osmotic water flux and 0.14 mM reverse solute flux and  $J_s/J_w$  of it is 3 times lower than that of pure CA. The modified membrane shown better properties compared with some commercial membranes. This simple way to fabricate FO membrane may have wide application prospect in the wastewater treatment and water purification.

**Acknowledgements** This work is financed by the National Natural Science Foundation of China (No. 51603214, 51475450 and 51703235) and the China Postdoctoral Science Foundation funded project (2017 M612042).

## References

- Seader JD, Henley EJ, Roper DK (2011) Separation process principles: Chemical and biochemical operations
- Cath TY, Childress AE, Elimelech M (2006) Forward osmosis: principles, applications, and recent developments. *J Membr Sci* 281(1–2):70–87
- Zhao S, Zou L, Tang CY, Mulcahy D (2012) Recent developments in forward osmosis: opportunities and challenges. *J Membr Sci* 396(1):1–21
- Achilli A, Childress AE, Cath TY (2009) Power generation with pressure retarded osmosis: an experimental and theoretical investigation. *J Membr Sci* 343(1–2):42–52
- Kravath RE, Davis JA (1975) Desalination of sea water by direct osmosis. *Desalination* 16(2):151–155
- Mccutcheon JR, Mccinnis RL, Elimelech M (2005) A novel ammonia-carbon dioxide forward (direct) osmosis desalination process. *Desalination* 174(1):1–11
- Cornelissen ER, Harmsen D, Korte KFD, Ruiken CJ, Qin JJ, Oo H, Wessels LP (2008) Membrane fouling and process performance of forward osmosis membranes on activated sludge. *J Membr Sci* 319(1–2):158–168
- Martinetti CR, Childress AE, Cath TY (2009) High recovery of concentrated RO brines using forward osmosis and membrane distillation. *J Membr Sci* 331(1–2):31–39
- Cornelissen ER, Harmsen D, Beerendonk EF, Qin JJ, Oo H, de Korte KF, Kappelhof JW (2011) The innovative osmotic membrane bioreactor (OMBR) for reuse of wastewater. *Water Sci Technol* 63(8): 1557–1565
- Petrots KB, Quantick P, Petropakis H, Petrots KB, Quantick P, Petropakis H (1998) A study of the direct osmotic concentration of tomato juice in tubular membrane-module configuration. I The effect of certain basic process parameters on the process performance *J Membr Sci* 150(1):99–110
- Petrots KB, Lazarides HN (2001) Osmotic concentration of liquid foods. *J Food Eng* 49(2):201–206
- Hoover LA, Phillip WA, Tiraferri A, Yip NY, Elimelech M (2011) Forward with osmosis: emerging applications for greater sustainability. *Environ Sci Technol* 45(23):9824–9830

13. McGinnis RL, Elimelech M (2009) Global challenges in energy and water supply: the promise of engineered osmosis. *Environ Sci Technol* 42(23):8625–8629
14. Gu Y, Chen L, Ng JW, Lee C, Chang WC, Tang CY (2015) Development of anaerobic osmotic membrane bioreactor for low-strength wastewater treatment at mesophilic condition. *J Membr Sci* 490:197–208
15. Wang KY, Chung TS, Qin JJ (2007) Polybenzimidazole (PBI) nanofiltration hollow fiber membranes applied in forward osmosis process. *J Membr Sci* 300(1–2):6–12
16. Yang Q, Wang KY, Chung TS (2009) Dual-layer hollow fibers with enhanced flux as novel forward osmosis membranes for water production. *Environ Sci Technol* 43(8):2800–2805
17. Kai YW, Rui CO, Chung TS (2010) Double-skinned forward osmosis membranes for reducing internal concentration polarization within the porous sublayer. *Ind Eng Chem Res* 49(10):4824–4831
18. Wang R, Shi L, Tang CY, Chou S, Qiu C, Fane AG (2010) Characterization of novel forward osmosis hollow fiber membranes. *J Membr Sci* 355(1–2):158–167
19. Yip NY, Tiraferri A, Phillip WA, Schiffman JD, Elimelech M (2010) High performance thin-film composite forward osmosis membrane. *Environ Sci Technol* 44(10):3812–3818
20. Shuren C, Shi L, Wang R, Tang CY, Qiu CQ, Fane AG, Hasson D (2010) Characteristics and potential applications of a novel forward osmosis hollow fiber membrane. *Desalination* 261(3):365–372
21. Su J, Zhang S, Chen H, Chen H, Jean YC, Chung TS (2010) Effects of annealing on the microstructure and performance of cellulose acetate membranes for pressure-retarded osmosis processes. *J Membr Sci* 364(1–2):344–353
22. Ren J, Mccutcheon JR (2014) A new commercial thin film composite membrane for forward osmosis. *Desalination* 343(12):187–193
23. Wang KY, Chung TS, Amy G (2012) Developing thin-film-composite forward osmosis membranes on the PES/SPSf substrate through interfacial polymerization. *AIChE J* 58(3):770–781
24. Wang Y, Li X, Cheng C, He Y, Pan J, Xu T (2016) Second interfacial polymerization on polyamide surface using aliphatic diamine with improved performance of TFC FO membranes. *J Membr Sci* 498(15):30–38
25. Arribas P, Khayet M, García-Payo MC, Gil L (2014) Self-sustained electro-spun polysulfone nano-fibrous membranes and their surface modification by interfacial polymerization for micro- and ultra-filtration. *Sep Purif Technol* 1138(138):118–129
26. Seman MNA, Khayet M, Hilal N (2011) Development of antifouling properties and performance of nanofiltration membranes modified by interfacial polymerisation. *Desalination* 273(1):36–47
27. Tsai CW, Tsai C, Ruaan RC, Hu CC, Lee KR (2013) Interfacially polymerized layers for oxygen enrichment: a method to overcome Robeson's upper-bound limit. *ACS Appl Mater Inter* 5(12):5563–5568
28. Duarte AP, Cidade MT, Bordado JC (2006) Cellulose acetate reverse osmosis membranes: optimization of the composition. *Sep Purif Technol* 100(5):4052–4058
29. Idris A, Ismail AF, Noordin MY, Shilton SJ (2002) Optimization of cellulose acetate hollow fiber reverse osmosis membrane production using Taguchi method. *J Membr Sci* 205(1–2):223–237
30. Vásárhelyi K, Ronner JA, Mulder MHV, Smolders CA (1987) Development of wet-dry reversible reverse osmosis membrane with high performance from cellulose acetate and cellulose triacetate blend. *Desalination* 61(3):211–235
31. Zhang C, Ou Y, Lei WX, Wan LS, Ji J, Xu ZK (2016) CuSO<sub>4</sub>/H<sub>2</sub>O<sub>2</sub>-induced rapid deposition of polydopamine coatings with high uniformity and enhanced stability. *Angew Chem Int Edit* 55(9):3106–3109
32. Yang FK, Zhao B (2011) Adhesion properties of self-polymerized dopamine thin film. *Open Sur Sci J* 3(1):115–122
33. Lee H, Scherer NF, Messersmith PB (2006) Single-molecule mechanics of mussel adhesion. *Proc Natl Acad Sci U S A* 103(35):12999–13003
34. Lee H, Dellatore SM, Miller WM, Messersmith PB (2007) Mussel-inspired surface chemistry for multifunctional coatings. *Science* 318(5849):426–430
35. Bui NN, McCutcheon JR (2013) Hydrophilic nanofibers as new supports for thin film composite membranes for engineered osmosis. *Environ Sci Technol* 47(3):1761–1769
36. Hancock NT, Cath TY (2009) Solute coupled diffusion in osmotically driven membrane processes. *Environ Sci Technol* 43(17):6769–6775
37. She Q, Jin X, Tang CY (2012) Osmotic power production from salinity gradient resource by pressure retarded osmosis: effects of operating conditions and reverse solute diffusion. *J Membr Sci* 401–402:262–273
38. Zheng Y, Huang MH, Chen L, Zheng W, Xie PK, Xu Q (2015) Comparison of tetracycline rejection in reclaimed water by three kinds of forward osmosis membranes. *Desalination* 359:113–122